JACS
JOURNAL OF THE AMERICAN CHEMICAL SOCIETY

Communication

pubs.acs.org/JACS

Evidence That the β Subunit of *Chlamydia trachomatis* Ribonucleotide Reductase Is Active with the Manganese Ion of Its Manganese(IV)/Iron(III) Cofactor in Site 1

Laura M. K. Dassama,[†,#] Amie K. Boal,[§,#] Carsten Krebs,*[,†,‡] Amy C. Rosenzweig,*[,§] and J. Martin Bollinger, Jr.*[,†,‡]

Departments of [†]Biochemistry and Molecular Biology and [‡]Chemistry, The Pennsylvania State University, University Park, Pennsylvania 16802, United States

[§]Departments of Molecular Biosciences and Chemistry, Northwestern University, Evanston, Illinois 60208, United States

Supporting Information

ABSTRACT: The reaction of a class I ribonucleotide reductase (RNR) begins when a cofactor in the β subunit oxidizes a cysteine residue ~35 Å away in the α subunit, generating a thiyl radical. In the class Ic enzyme from *Chlamydia trachomatis* (*Ct*), the cysteine oxidant is the Mn^{IV} ion of a Mn^{IV}/Fe^{III} cluster, which assembles in a reaction between O_2 and the Mn^{II}/Fe^{II} complex of β. The heterodinuclear nature of the cofactor raises the question of which site, 1 or 2, contains the Mn^{IV} ion. Because site 1 is closer to the conserved location of the cysteine-oxidizing tyrosyl radical of class Ia and Ib RNRs, we suggested that the Mn^{IV} ion most likely resides in this site (i.e., $^{1}Mn^{IV}/^{2}Fe^{III}$), but a subsequent computational study favored its occupation of site 2 ($^{1}Fe^{III}/^{2}Mn^{IV}$). In this work, we have sought to resolve the location of the Mn^{IV} ion in *Ct* RNR-β by correlating X-ray crystallographic anomalous scattering intensities with catalytic activity for samples of the protein reconstituted *in vitro* by two different procedures. In samples containing primarily Mn^{IV}/Fe^{III} clusters, Mn preferentially occupies site 1, but some anomalous scattering from site 2 is observed, implying that both $^{1}Mn^{II}/^{2}Fe^{II}$ and $^{1}Fe^{II}/^{2}Mn^{II}$ complexes are competent to react with O_2 to produce the corresponding oxidized states. However, with diminished Mn^{II} loading in the reconstitution, there is no evidence for Mn occupancy of site 2, and the greater activity of these "low-Mn" samples on a per-Mn basis implies that the $^{1}Mn^{IV}/^{2}Fe^{III}$-β is at least the more active of the two oxidized forms and may be the only active form.

In the remarkable first step in the reaction of a class I ribonucleotide reductase (RNR), an oxidizing equivalent or "hole" migrates ~35 Å from its resting location in the interior of the cofactor subunit, β, onto a cysteine residue in the active site of the catalytic subunit, α,[1,2] where the nascent cysteine thiyl radical abstracts hydrogen ($H^{\bullet}$) from the 3′ carbon of the substrate to initiate the reduction of its 2′ carbon.[3−6] During translocation of the hole, aromatic residues in a specific pathway are transiently oxidized to radicals in shorter "electron-hopping" steps.[5,6] In the most extensively studied class I RNR, the Ia enzyme from *Escherichia coli* (*Ec*), the resting location of the hole is Y122,[7,8] which is oxidized to a tyrosyl radical ($Y^{\bullet}$) in an auto-activation reaction between the nearby non-heme $Fe_2^{II/II}$ cluster and O_2.[9−11] The $Y^{\bullet}$ is asymmetrically disposed with respect to the μ-oxo-$Fe_2^{III/III}$ co-product of the activation reaction, positioned closer to metal site 1, which, in turn, is the closer of the two sites to W48 of the hole-transfer pathway.[12] Whereas the use of a $Y^{\bullet}$ is conserved among class Ia[10,11] and Ib[13,14] RNRs, the class Ic enzyme from *Chlamydia trachomatis* (*Ct*) instead stores the hole directly on the metallocofactor, a stable, high-valent heterodinuclear Mn^{IV}/Fe^{III} cluster that is reduced to Mn^{III}/Fe^{III} upon hole migration.[15−19] Analogously to the $Y^{\bullet}$-generating activation step of the *Ec* Ia enzyme,[10,11] the *Ct* RNR cofactor assembles in a reaction between the reduced dimetal cluster (Mn^{II}/Fe^{II}) and O_2.[20]

The presence of two different metals in the *Ct* RNR cofactor raises a number of questions regarding its formation and function. Most importantly, must the Mn^{IV} of the active state reside specifically in site 1 or 2 or, alternatively, can it function ambiguously in either site? The initial structure of the *Ct* β protein did not resolve this question, because it was solved before the Mn requirement of the enzyme had been revealed and is assumed to have been of the inactive $Fe_2^{III/III}$ complex.[21] Under the presumption that only one of the two possible Mn^{IV}/Fe^{III} forms would be active, we previously suggested that the Mn^{IV} occupies site 1, putting it closer to the known location of the hole (the $Y^{\bullet}$) in the class Ia and Ib enzymes and in line with the pathway W residue (W51).[18] This speculative site assignment seemed to be supported by a subsequent report on a structurally similar Mn/Fe protein, a ligand-binding putative oxidase from *Mycobacterium tuberculosis*, in which the location of the Mn was shown by X-ray crystallographic anomalous scattering experiments to be site 1,[22] and by a computational study on the *Ct* RNR itself.[23] However, a more recent computational study suggested that the Mn^{IV} ion might reside in site 2.[24]

In *Ct* cells, assembly factors (e.g., metallochaperones) could specify the location of the Mn^{IV}, but in the heterologous expression and/or *in vitro* reconstitution procedures employed in all studies on the *Ct* RNR reported to date,[15,25,26] the location of the Mn^{IV} should be dictated by a combination of (i)

Received: December 2, 2011
Published: January 12, 2012

   dx.doi.org/10.1021/ja211314p | *J. Am. Chem.Soc.* 2012, 134, 2520−2523

the thermodynamics and kinetics of Mn^{II} and Fe^{II} binding to the two sites (i.e., their relative metal-binding affinities, their specificities for Fe^{II} *vs* Mn^{II}, and their corresponding on- and off-rates), (ii) the reactivity of the two possible forms of the labile Mn^{II}/Fe^{II} cluster, $^{1}Mn^{II}/^{2}Fe^{II}$ and $^{1}Fe^{II}/^{2}Mn^{II}$ (denoting Mn in site 1 or 2, respectively), toward O_2, and (iii) the conditions under which the Mn/Fe cofactor is assembled. For example, in the activation procedure that we have employed in previous studies[26] (procedure **1**), Mn^{II} is added to apo β at a Mn/β ratio (1.5) similar to the experimentally determined stoichiometry of functional metal sites (~1.4; as for the *Ec* β protein, it is not clear why the number of functional sites is less that the theoretical value of 2). Half this quantity of Fe^{II} (0.75 equiv) is subsequently slowly infused over several minutes in the presence of excess O_2, and weakly bound or unbound metal ions are then removed by dialysis of the sample against EDTA. The expectation is that Mn^{II} should initially fill all or nearly all of the metal sites, forming the O_2-inert $Mn_2^{II/II}$-β complex. Upon addition of limiting Fe^{II}, it should (if Fe^{II} on-rates for the *Ct* protein are comparable to values reported for the *Ec* protein) rapidly bind to sites vacated by the labile Mn^{II}, forming either $^{1}Mn^{II}/^{2}Fe^{II}$-β or $^{1}Fe^{II}/^{2}Mn^{II}$-β. The O_2-reactive form(s) should then be trapped to produce the corresponding oxidized state(s).

A sample prepared by this procedure **1** [1.50 Mn/β added and 0.55 retained, as determined by inductively coupled plasma atomic emission spectroscopy (ICP-AES) after removal of unbound metal ions, Table S1] was crystallized (PDB accession code 4D8F) in preparation for X-ray diffraction experiments to address the location of the Mn. In contrast to the crystals previously used to determine the structure of the $Fe_2^{III/III}$ protein, which had only one β monomer per asymmetric unit (ASU),[21] these Mn/Fe forms of the protein crystallized with either one or two dimers (two or four β monomers) in the ASU (Table S2). Thus, the diffraction data on these crystals afford six independent views of the cofactor site. Diffraction data collected at the Mn absorption edge show that Mn preferentially occupies site 1 of the cluster site. Figure 1A shows the Mn anomalous difference density at the active site in a representative monomer. In all six views of the cofactor site, the Mn anomalous scattering peak at site 1 is more intense than

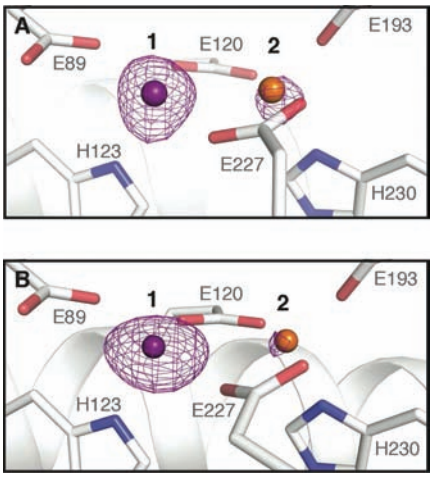

Figure 1. Anomalous difference electron density maps for procedure **1** (A) and procedure **2** (B) samples. Maps representing data collected at the Mn absorption edge (6.68 keV) are shown in purple mesh (contoured at 5.5σ).

Table 1. Anomalous Peak Heights at the Mn Absorption Edge

Sample	Chain	Site 1	Site 2
procedure **1**	A	9.8	6.8
crystal form 1	B	9.5	5.2
	C	10.2	5.2
	D	7.1	2.0
procedure **1**	A	12.9	7.3
crystal form 2	B	10.3	7.9
procedure **2**	A	14.5	5.9
	B	12.7	5.2
	C	11.9	4.8
	D	8.7	5.0

that at site 2 (Table 1). However, in two separate data sets, Mn occupancy of site 2 is evident in at least one monomer in the ASU (anomalous density > 6.0σ).

To further investigate this apparent preferential occupancy of site 1 by Mn, a second sample was prepared by the initial addition of limiting Mn^{II} followed by the rapid addition of excess Fe^{II} in the presence of excess O_2 (procedure **2**; PDB accession code 4D8G). In this protocol, low Mn^{II}/β ratios should maximize differential site occupancy arising from any difference between the intrinsic affinities of the two sites. The corresponding data taken on crystals of this sample (0.3 Mn/β added and 0.22 retained, Table S1), yield a Mn anomalous difference map indicative of far less occupancy of site 2 and increased contrast between sites 1 and 2 (Figure 1B and Table 1). The Mn anomalous scattering data thus imply that site 1 is preferentially occupied by Mn following both *in vitro* reconstitution procedures and that this preference is greater when the reaction is performed using limiting Mn^{II}.

To gain information about the Fe content of each site, data sets were also collected at 7.2 keV. In the sample from procedure **1**, anomalous difference amplitude maps[27] (Figure S1) suggest significant Fe occupancy only of site 2. In the procedure **2** sample with less Mn and excess Fe, the Fe scattering is still more intense at site 2, but significant occupancy of site 1 is also observed (Figure S1). Thus, the Fe edge data suggest a preference for site 2, particularly when site 1 is initially fully occupied by Mn^{II} in the activation process.

The highest resolution data sets for each procedure were solved and fully refined (Tables S2 and S3). In addition to the crystal-packing differences noted above, minor differences from the published structure of the $Fe_2^{III/III}$ form could be noted (Figure S2). Although the data sets are of sufficiently high resolution (1.75−2.40 Å) to visualize structural detail at the cofactor sites (Figure S3), the resulting models must necessarily be interpreted with caution. Because of heterogeneity in the occupancy of Mn vs Fe in site 2 in the procedure **1** structures and low overall metal occupancy in the procedure **2** structure (Figure S3), it is difficult to definitively model the positions of side chains and bridging ligands. Additionally, the oxidation states of the metals in the final structures are unknown because the Mn^{IV}/Fe^{III} cluster has been shown to undergo both adventitious reduction on the time scale of crystallization and X-ray photoreduction during data collection.[28]

dx.doi.org/10.1021/ja211314p | *J. Am. Chem.Soc.* 2012, 134, 2520−2523

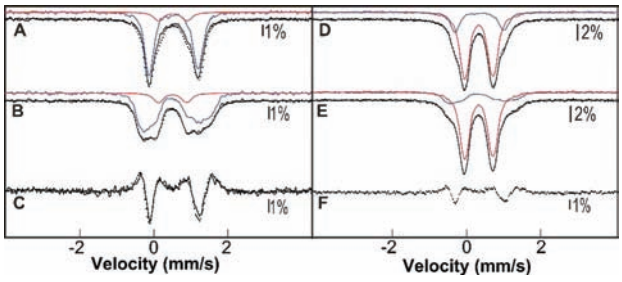

Figure 2. Mössbauer spectra of the procedures **1** (A–C) and **2** (D–F) samples. Spectra were collected at 4.2 K with externally applied magnetic fields of 0 mT (A,D) or 53 mT (B,E). (C,F) The corresponding difference spectra. The red and blue solid lines are "reference spectra" of the $Fe_2^{III/III}$ and Mn^{IV}/Fe^{III} forms, respectively. The solid black lines represent the summed contribution of these two components. The ~10% contribution of the Mn^{III}/Fe^{III} form has been removed from the spectrum shown in spectrum E (see Figures S4 and S6). The solid line in spectrum C is the difference spectrum of the procedure **2** sample, multiplied by 3.5 and shown for comparison.

To investigate the origin of the crystallographically observed differences in the Mn and Fe occupancies, replicate samples were prepared by procedures **1** and **2**, the quantities of Mn and Fe retained in the samples were determined by ICP-AES (Table S1), and the various cluster forms were quantified by a combination of Mössbauer and EPR spectroscopies. The Mössbauer spectra of the procedure **1** sample (Figure 2A, B) exhibit the field-dependence typical of the stable heterodinuclear Mn^{IV}/Fe^{III} cluster.[16] Analysis of the spectra reveals that the sample contains ~75% of total Fe in Mn^{IV}/Fe^{III} clusters. In addition, the sample contains small quantities of $Fe_2^{III/III}$ and Mn^{III}/Fe^{III} clusters (~11% of total Fe in each). The magnetically split features of the Mn^{III}/Fe^{III} clusters are seen in the 4.2 K/53 mT spectrum collected over a wider range of Doppler velocities (Figure S4) and the X-band EPR spectrum of this sample (Figure S5A). The spectroscopic analyses reveal the presence of 0.45 equiv Mn^{IV}/Fe^{III}, 0.07 equiv Mn^{III}/Fe^{III}, and 0.03 equiv of $Fe_2^{III/III}$. The Mn^{IV}/Fe^{III} and Mn^{III}/Fe^{III} forms thus account for all of the Mn in the procedure **1** sample, implying that the Mn anomalous scattering from site 2 arises from the $^1Fe^{III}/^2Mn^{IV}$ form and, therefore, that both the $^1Fe^{II}/^2Mn^{II}$ and $^1Mn^{II}/^2Fe^{II}$ forms of *Ct* β may be reactive toward O_2.

The Mössbauer spectra of the procedure **2** sample (Figure 2D, E) are dominated by the quadrupole doublet associated with the $Fe_2^{III/III}$ complex (78 ± 3% of total Fe, red lines), as expected in view of the excess of Fe^{II} over Mn^{II} used in activating the protein. The remaining 22 ± 3% of spectral intensity exhibits the dependence on the magnitude of the externally applied magnetic field that characterizes the S = 1 Mn^{IV}/Fe^{III} state (Figure 2E).[16] The fact that a lesser fraction of the intensity exhibits this dependence implies that the sample contains a smaller fraction of Mn^{IV}/Fe^{III} clusters. The X-band EPR spectrum of this sample (Figure S5B) further reveals a small quantity, less than the detection limit of Mössbauer spectroscopy, of the Mn^{III}/Fe^{III} form. Thus, the sample contains 0.25 equiv (78% of 0.65 equiv Fe/2 Fe per cluster) $Fe_2^{III/III}$ clusters and 0.15 equiv of Mn^{IV}/Fe^{III} clusters. The quantity of Fe in the form of Mn^{IV}/Fe^{III} clusters determined by Mössbauer spectroscopy agrees well with the quantity of Mn determined independently by ICP-AES (Table S1), thereby demonstrating that ~95% of the Mn is in the oxidized state. These findings are consistent with the observation of Fe in both sites (Figure S1).

The ICP-AES, X-ray anomalous diffraction, Mössbauer, and EPR data on these samples together suggest that both possible forms of the Mn^{IV}/Fe^{III} cluster ($^1Mn^{IV}/^2Fe^{III}$ and $^1Fe^{III}/^2Mn^{IV}$) are produced from the corresponding reduced states by reaction with O_2, with the $^1Mn^{IV}/^2Fe^{III}$ cluster being formed preferentially. In principle, these two oxidized forms might be distinguishable spectroscopically, but the Mössbauer data do not suggest even partial resolution of features attributable to the two different forms. However, treatment of these two samples with an excess of dithionite reduces the Mn^{IV}/Fe^{III} cluster(s) to the S = 1/2 Mn^{III}/Fe^{III} state(s) (Figure S5C, D). The EPR difference spectra showing the changes resulting from reduction of the procedures **1** and **2** samples (Figure S5E) are markedly different. Specific attribution of EPR features to different forms of the Mn^{III}/Fe^{III} cluster will require more extensive correlation of spectral differences with differences in activation method. Nevertheless, the documented differences correlated to activation procedure lend credence to the notion that both possible Mn^{IV}/Fe^{III} clusters can form. This conclusion raises the question of which form(s) is (are) active.

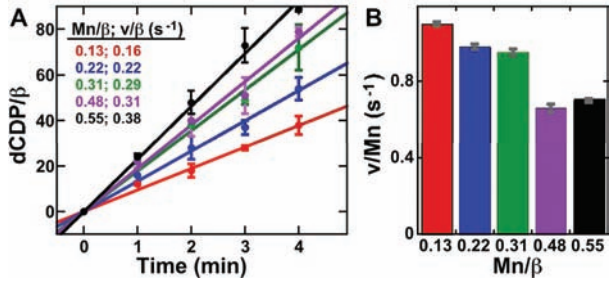

Figure 3. Comparison of the RNR activities of samples reconstituted by procedure **1** (black symbols and lines; see Supporting Information for preparation and assay conditions) and procedure **2** with varying amounts of Mn (red, blue, green and purple symbols and lines). (A) Equivalents of dCDP produced as a function of time. The quantity of Mn per β and velocity/β (dCDP/s/β) are shown color-coded in the inset. (B) Velocity of dCDP production per Mn as a function of Mn per β. Bars are colored according to the labels in the inset of A.

The RNR activities of a sample of *Ct* β reconstituted by procedure **1** and a series of samples reconstituted by procedure **2** (with the added Mn^{II}/β ratio varied from 0.15 to 0.6, Table S1) were determined by a previously published mass spectrometric assay (Figures 3A and S7A). Activity increases with the quantity of Mn retained (measured by ICP-AES after removal of unbound metal ions). This trend is expected: only the Mn/Fe form of *Ct* β has activity; the $Fe_2^{III/III}$ complex that is the predominant product with low Mn^{II}/β and high Fe^{II}/β in procedure **2** is inactive. The more informative trend is observed in comparison of the activity of the samples on a per Mn basis (Figures 3B and S7B). This value decreases with increasing Mn/β across the series of samples prepared by procedure **2** (colored bars). The activity/Mn of the sample prepared by procedure **1** (black) is approximately equal to that of the procedure **2** sample prepared with greatest Mn^{II}/β (0.48, purple). Given that the anomalous difference maps imply greater Mn site 2 occupancy following procedure **1** (with the greatest Mn^{II}/β of all the samples), the fact that the samples prepared by procedure **2** and employing the least Mn^{II}/β have the greatest activity/Mn implies that the $^1Mn^{IV}/^2Fe^{III}$ form is at

least more active than the $^{1}Fe^{III}/^{2}Mn^{IV}$ form. Definitive determination of whether the latter form is merely less active or is completely inactive will require both further optimization of reconstitution procedures to maximize yields of either form and identification of specific spectral features that can be used to assess the product distribution more quantitatively.

A very recent study by Högbom and co-workers also addressed the location of the Mn ion by X-ray crystallographic anomalous diffraction measurements.[29] Their overall conclusion that Mn occupies site 1 is consistent with our results. However, the use of protein prepared by *Ec* over-expression in Mn-supplemented medium without any further treatment to enrich in the active state, the absence of any assessment of the nature and distribution of cluster forms, and, most importantly, the relatively low activity/Mn of the samples (≤35% of the *minimum* value in our study) underscores the need for the correlation of site occupancy to catalytic activity. In addition, their conclusion that Mn resides exclusively in site 1 would imply a remarkable specificity imposed either intrinsically by the *Ct* β protein or by fortuitous metal loading in the heterologous expression host. By contrast, our conclusions suggest a more modest selectivity, perhaps hinting that the native host might possess specialized assembly factors to direct formation of the correct cluster form. Regardless, experimentally addressing the magnitude and basis of the Mn^{II} vs Fe^{II} selectivity of the cluster sites will be critical to understanding how the class Ic β protein properly assembles its novel cofactor.

■ ASSOCIATED CONTENT

Ⓢ Supporting Information

Description of reconstitution procedures; metal content of all samples; general crystallographic methods and refinement statistics for both structures; additional anomalous difference maps; diagram of crystal packing interactions between the two β dimers; electron density maps at the cofactor sites of a representative β_2; Mössbauer spectrum of the procedure **1** sample collected over a wider range of Doppler velocities; X-band EPR spectra of the procedures **1** and **2** samples. This material is available free of charge via the Internet at http://pubs.acs.org.

■ AUTHOR INFORMATION

Corresponding Author

ckrebs@psu.edu; amyr@northwestern.edu; jmb21@psu.edu

Author Contributions

[#]These authors contributed equally to this work.

Notes

The authors declare no competing financial interest.

■ ACKNOWLEDGMENTS

This work was supported by the National Institutes of Health (GM-55365 to CK and JMB, GM58518 to ACR, and an NRSA to AKB). Use of the Advanced Photon Source was supported by the U.S. Department of Energy, Office of Science, Office of Basic Energy Sciences, under Contract No. DE-AC02-06CHII357. Use of the LS-CAT Sector 21 was supported by the Michigan Economic Development Corporation and the Michigan Technology Tri-Corridor (Grant 085P1000817). GM/CA-CAT has been funded in whole or in part with Federal funds from the National Cancer Institute (Y1-CO-1020) and the National Institute of General Medical Sciences (Y1-GM-1104). We thank Taeho Lim for technical assistance.

■ REFERENCES

(1) Uhlin, U.; Eklund, H. *Nature* **1994**, *370*, 533−539.
(2) Bennati, M.; Robblee, J. H.; Mugnaini, V.; Stubbe, J.; Freed, J. H.; Borbat, P. *J. Am. Chem. Soc.* **2005**, *127*, 15014−15015.
(3) Mao, S. S.; Holler, T. P.; Yu, G. X.; Bollinger, J. M. Jr.; Booker, S.; Johnston, M. I.; Stubbe, J. *Biochemistry* **1992**, *31*, 9733−9743.
(4) Mao, S. S.; Yu, G. X.; Chalfoun, D.; Stubbe, J. *Biochemistry* **1992**, *31*, 9752−9759.
(5) Stubbe, J.; Nocera, D. G.; Yee, C. S.; Chang, M. C. Y. *Chem. Rev.* **2003**, *103*, 2167−2202.
(6) Reece, S. Y.; Hodgkiss, J. M.; Stubbe, J.; Nocera, D. G. *Philos. Trans. R. Soc., B* **2006**, *361*, 1351−1364.
(7) Atkin, C. L.; Thelander, L.; Reichard, P.; Lang, G. *J. Biol. Chem.* **1973**, *248*, 7464−7472.
(8) Sjöberg, B.-M.; Reichard, P.; Gräslund, A.; Ehrenberg, A. *J. Biol. Chem.* **1977**, *252*, 536−541.
(9) Bollinger, J. M. Jr.; Edmondson, D. E.; Huynh, B. H.; Filley, J.; Norton, J. R.; Stubbe, J. *Science* **1991**, *253*, 292−298.
(10) Stubbe, J. *Curr. Opin. Chem. Biol.* **2003**, *7*, 183−188.
(11) Nordlund, P.; Reichard, P. *Annu. Rev. Biochem.* **2006**, *75*, 681−706.
(12) Nordlund, P.; Sjöberg, B.-M.; Eklund, H. *Nature* **1990**, *345*, 593−598.
(13) Cotruvo, J. A. Jr.; Stubbe, J. *Biochemistry* **2010**, *49*, 1297−1309.
(14) Cox, N.; Ogata, H.; Stolle, P.; Reijerse, E.; Auling, G.; Lubitz, W. *J. Am. Chem. Soc.* **2010**, *132*, 11197−11213.
(15) Jiang, W.; Yun, D.; Saleh, L.; Barr, E. W.; Xing, G.; Hoffart, L. M.; Maslak, M.-A.; Krebs, C.; Bollinger, J. M. Jr. *Science* **2007**, *316*, 1188−1191.
(16) Jiang, W.; Bollinger, J. M. Jr.; Krebs, C. *J. Am. Chem. Soc.* **2007**, *129*, 7504−7505.
(17) Jiang, W.; Yun, D.; Saleh, L.; Bollinger, J. M. Jr.; Krebs, C. *Biochemistry* **2008**, *47*, 13736−13744.
(18) Bollinger, J. M. Jr.; Jiang, W.; Green, M. T.; Krebs, C. *Curr. Opin. Struct. Biol.* **2008**, *18*, 650−657.
(19) Jiang, W.; Xie, J.; Varano, P. T.; Krebs, C.; Bollinger, J. M. Jr. *Biochemistry* **2010**, *49*, 5340−5349.
(20) Jiang, W.; Hoffart, L. M.; Krebs, C.; Bollinger, J. M. Jr. *Biochemistry* **2007**, *46*, 8709−8716.
(21) Högbom, M.; Stenmark, P.; Voevodskaya, N.; McClarty, G.; Gräslund, A.; Nordlund, P. *Science* **2004**, *305*, 245−248.
(22) Andersson, C. S.; Högbom, M. *Proc. Natl. Acad. Sci. U.S.A.* **2009**, *106*, 5633−5638.
(23) Roos, K.; Siegbahn, P. E. M. *Biochemistry* **2009**, *48*, 1878−1887.
(24) Han, W. G.; Giammona, D. A.; Bashford, D.; Noodleman, L. *Inorg. Chem.* **2010**, *49*, 7266−7281.
(25) Voevodskaya, N.; Lendzian, F.; Ehrenberg, A.; Gräslund, A. *FEBS Lett.* **2007**, *581*, 3351−3355.
(26) Jiang, W.; Xie, J.; Nørgaard, H.; Bollinger, J. M. Jr.; Krebs, C. *Biochemistry* **2008**, *47*, 4477−4483.
(27) Than, M. E.; Henrich, S.; Bourenkov, G. P.; Bartunik, H. D.; Huber, R.; Bode, W. *Acta Crystallogr.* **2005**, *D61*, 505−12.
(28) Younker, J. M.; Krest, C. M.; Jiang, W.; Krebs, C.; Bollinger, J. M. Jr.; Green, M. T. *J. Am. Chem. Soc.* **2008**, *130*, 15022−15027.
(29) Andersson, C. S.; Öhrström, M.; Popović-Bijelić, A.; Gräslund, A.; Stenmark, P.; Högbom, M. *J. Am. Chem. Soc.* **2012**, *134*, 123−125.